SciMedCentral

JSM Nanotechnology & Nanomedicine

Research Article

Ionic Liquid-Assisted Fabrication of Nanoscale Microporous TiO_2 with Enhanced Photocatalytic Performance

Junbo Zhong[1,2]*, Jianzhang Li[1], Famei Feng[1], Shengtiang Huang[1], Weidong Jiang[1] and Clemens Burda[2]*

[1]*Key Laboratory of Green Catalysis of Higher Education Institutes of Sichuan, College of Chemistry and Pharmaceutical Engineering, Sichuan University of Science and Engineering, China*

[2]*Department of Chemistry, Case Western Reserve University, USA*

Corresponding author

Clemens Burda, Department of Chemistry, Case Western Reserve University, 10900 Euclid Avenue, Cleveland, Ohio 44106, USA, Tel: 216 368 5918; Email: burda@case.edu

Submitted: 13 August 2013

Accepted: 23 September 2013

Published: 25 September 2013

Keywords

- $NTiO_2$
- Photocatalytic property
- Ionic liquid
- Surface photovoltage spectroscopy
- Micropores

Abstract

In this work, microporous TiO_2 photocatalyst (IL-TiO_2) with high photocatalytic performance was prepared via a sol-gel method using the ionic solvent 1-butyl-3-methylimidazolium hexafluorophosphate ([BMIm]PF_6). The specific surface area, structure, morphology, the surface hydroxyl content, the photoinduced charge separation efficiency and the transport of the photogenerated charges of the photocatalysts prepared were characterized by Brunauer-Emmett-Teller (BET) measurements, X-ray diffraction (XRD), scanning electron microscopy (SEM), X-ray photoelectron spectroscopy (XPS) and surface photovoltage spectroscopy (SPS) studies, respectively. The results show that adding [BMIm]PF_6 into the synthesis alters the specific surface parameters, the morphology and the transport of the photogenerated charges. It increases the hydroxyl content on the surface of TiO_2. The photocatalytic activity toward decolorization of methyl orange (MO) aqueous solution was investigated. The results demonstrate that the photocatalytic activity of IL-TiO_2 is more than 22 times that of the reference TiO_2 and the underlying mechanisms are discussed.

INTRODUCTION

As an advanced oxidation process, photocatalysis has received a great deal of attention for wastewater treatment and air purification in recent years [1-4]. Among the various photocatalysts, TiO_2 based photocatalysts have been intensely investigated [5-9]. However, its wide band gap, high recombination rate of electron and hole pair, and the slow transfer rate of electrons to oxygen limit the practical application of TiO_2 photocatalyst [10,11]. Therefore, the photocatalytic performance of TiO_2 has to be further improved. Thus, enormous efforts have been developed to enhance the photocatalytic activity of TiO_2 to meet the practical demands. Many synthesis methods have been pursued to promote the photocatalytic activity of TiO_2 [12-15]. Among these synthesis approaches, the sol-gel method has been widely employed due to the low cost of the equipment required and the resulting high purity of the products [16].

More recently, room-temperature ionic liquids (RTILs) have attracted significant attention as a new kind of reaction media [7,17]. RTILs have following attractive advantages: high ionic conductivity, good thermal stability, good dissolving ability, wide electrochemical window, nonflammability and negligible vapor pressure [18-21]. More importantly, the self-structuring of RTILs originating from the extended H-bond systems makes RTILs suitable as template for the synthesis of inorganic materials with ultrafine structure [20,22-23]. Compared to traditional surfactants, the outstanding physicochemical properties, such as tunable solvent features, adjustable polarities, and low vapor pressures, make RTILs more diverse in shape control and for a wide range of operating conditions [24-26]. As a result, new catalysts with new properties are now synthetically accessible.

Here, we present a study on the synthesis of an RTIL-prepared TiO_2 photocatalyst and its light-induced surface photovoltage (SPV) response. Surface photovoltage spectroscopy (SPS) method is a well-established nondestructive technique for semiconductor characterization that detects and analyzes illumination-induced changes in the surface photovoltage [27]. It is an effective and useful approach for investigating the photoexcited states of photocatalysts.

The primary goals of this work is to study the effect of [BMIm]PF_6 on the morphology, surface texture, the hydroxyl content, bandgap, the photoinduced charge separation and their relation to the photocatalytic activity of the prepared photocatalyst. The photocatalytic activity has been evaluated via the decolorization of methyl orange (MO) solution.

EXPERIMENTAL SECTION

Preparation of photocatalysts

[BMIm]PF_6 was purchased from Shanghai Chengjie Chemical Co. LTD. All other chemicals (analytical grade reagents) were supplied from the Chengdu Ke long Chemical Reagent Factory and used as received. TiO_2 was fabricated by the sol-gel process according to the procedure in reference [28]. 1g [BMIm]PF6 and Tetrabutylorthotitanate (17.2 mL), diethanolamine (4.8 mL) were dissolved in ethanol (67.3 mL). After stirring vigorously for 2 h at room temperature, a mixed solution of water (0.9 mL) and ethanol (10 mL) was added dropwise to the above solution under stirring. The resulting alkoxide solution was kept standing at room temperature for hydrolysis during 2 h, resulting in the TiO_2 sol. Then the TiO_2 sol was aged for one week at room temperature and air. Finally, the sample obtained was evaporated, dried, and baked in air at 723 K for 2 h in a muffle furnace. The sample was labeled as IL-TiO_2. TiO_2 was also prepared as the same procedure mentioned above without the presence of [BMIm]PF_6.

Characterization of photocatalysts

The specific surface area and pore size measurements were performed with a SSA-4200 automatic surface analyzer (Builder Inc., Beijing, China). The samples were evacuated at 623K for 1h, and then cooled to 77K using liquid N_2 at which point N_2 adsorption was measured. X-ray diffraction (XRD) patterns were recorded on a DX-2600 X-ray diffractometer (Fangyuan Inc., Dandong, China) using Cu Kα (λ = 0.15406 nm) radiation equipped with a graphite monochromator. The X-ray tube was operated at 40 kV and 25 mA. Scanning electron microscope (SEM) images were taken with a JSM-7500F scanning electron microscope (JEOL, Japan), using an accelerating voltage of 5 kV. The UV-Vis diffuse reflectance spectroscopy was performed on a TU-1907 spectrometer (Puxi Inc., Beijing, China) using barium sulphate as the reference. X-ray photoelectron spectroscopy (XPS) measurements were performed on XSAM800 (KRATOS, Great Britain) using the Mg K_α at 12 kV and 12 mA. The X-ray photoelectron spectra were referenced to the C_{1s} peak (*BE* = 284.80 eV) resulting from added graphite on the sample surface. The measurement error is ±0.10 eV for the standard sample. The surface photovoltage spectroscopy (SPS) measurements of the samples were carried out with a home-built apparatus based on the literature [29]. The instrument was made up of a source of monochromatic light, a lock-in amplifier (SR830-DSP) with a light chopper (SR540), and a photovoltaic cell interfaced with a computer [30]. Monochromatic light was provided by passing light from a 500 W xenon lamp (CHFXQ 500 W, Global Xenon Lamp Power) though an Omni-5007 grating monochromator (Zolix Inc., Beijing). The photovoltaic cell was a sandwich- structure of indium tin oxide ITO-sample-ITO. The change of surface potential in the presence of light and in the dark is the SPS signal. The raw SPS data were normalized with regard to light intensity using a Model Zolix UOM-1S illuminometer (Zolix Inc., Beijing).

Evaluation of the photocatalytic activity

Photocatalytic decolorization experiments were performed in a SGY-II photochemical reactor (Kaifeng HXSCI Science Instrument Factory, China). The radiation source was a 500 W high-pressure mercury lamp with a maximum emitting radiation at 365 nm, the lamp was encapsulated in a cooling quartz jacket and positioned in the middle of the reactor, two quartz test tubes were located around the lamp, the distance from the lamp to the quartz test tubes was 10 cm. The initial concentration of MO solution was 10 mg/L. 50 mg of prepared photocatalyst was added into 50 mL MO solution (10 mg/L) and the reaction mixture was continuously aerated with a pump to provide oxygen and also for the complete mixing of the reaction solution. The decolorization reaction was performed at room temperature. The pH value of the reaction solution was 7.0. At regular intervals, samples were withdrawn and centrifuged (6000 rpm) to separate photocatalyst from photoproducts for analysis. The concentration of MO was measured with a 756 PC spectrophotometer (Shun Yu Heng Ping Inc., Shanghai) at 460 nm using the Lambert-Beer law. Measurements have all been repeated at least three times.

RESULTS AND DISCUSSION

The specific surface parameters of the photocatalysts are shown in (Table 1). As shown in (Table 1), [BMIm]PF_6 changes greatly the specific surface parameters of TiO_2. The specific surface area increases from 72 m^2/g for TiO_2 to 121 m^2/g for IL-TiO_2, the pore volume also increases from 0.26 cc/g to 0.35 cc/g. The mean pore size decreases from 7.3 nm to 5.9 nm.

It is found that [BMIm]PF_6 greatly alters the distribution of the pores, as shown in (Figure 1). Appropriate distribution of the pores is beneficial to the diffusion of the reactants and products, which can help promote the photocatalytic performance. It is generally recognized that the photocatalytic process is related to the effective adsorption and desorption of molecules on the surface of the photocatalyst [31]. A high specific surface area can provide more reactive adsorption/desorption sites for photocatalytic reactions [32]. The photocatalytic performance benefits from a high surface area and an appropriate distribution of pores of the photocatalyst, this result can be further confirmed by the results of photocatalytic activity measurements presented below.

The XRD patterns of the photocatalysts prepared are shown in (Figure 2). As shown, all strong patterns can be indexed as pure anatase-type TiO_2 (JCPDS No. 89-4921). No other patterns can be observed, indicating high crystallinity of the as-prepared TiO_2 samples. Based on the XRD results, the crystallite size D of the photocatalysts was calculated using the Scherrer equation as follows: $D = K\lambda / \beta\cos\theta$, where λ is the wavelength of the X-ray radiation (λ = 0.154 nm), K is the Scherrer constant, a dimensionless shape factor K=0.89, and θ is the Bragg angle. β

Table 1: Surface parameter of the prepared photocatalysts.

photocatalyst	S_{BET} (m^2/g)	Pore volumes(cc/g)	Pore size(Å)
TiO_2	72 ± 3	0.26 ± 0.02	72.7 ± 3
IL-TiO_2	121 ± 5	0.35 ± 0.03	59.3 ± 2

is the line broadening at half the maximum intensity (FWHM), after subtracting the instrumental line broadening, in radians. From the equation, the crystal sizes of the IL-TiO_2 and TiO_2 were found to be 9 and 15 nm, respectively. This result illustrates that the increased crystal size leads to a decrease in BET surface area, which is consistent with the results of the BET surface area measurements.

The morphology of photocatalysts plays an important role in affecting the photocatalytic activity. The SEM images of photocatalysts prepared are shown in (Figure 3). As shown in (Figure 3), IL-TiO_2 looks rather irregular and porous, while TiO_2 appears less porous. In addition, the particle size of IL-TiO_2 is smaller than that of TiO_2. The microporous structure is attributed to the strong hydrogen bonds formed between the anions of the RTIL and the hydroxyl groups of the TiO_2 gel during the sol-gel process [34]. This may have caused the anions to be oriented along the pore walls and the cations to be aligned along with the anions because of the Coulomb interaction, molecular stacking via Van der Waals forces, or other noncovalent interactions between neighboring imidazolium rings [25,35-37]. Furthermore, the strong hydrogen bond formation is beneficial to produce uniformly adsorbed nuclei at the initial stage of the photocatalytic reaction. In general, the shape will greatly influence the chemistry and properties of nanomaterials [38]. This result can further be confirmed by the results of photocatalytic activity measurements.

It is commonly accepted that the UV-Vis diffuse absorption and reflection properties may have a strong effect on the photocatalytic activity. As shown in (Figure 4), the two photocatalysts have similar UV-Vis diffuse reflectance spectra, which demonstrates that [BMIm]PF_6 is not effectively changing the band-gap of TiO_2.

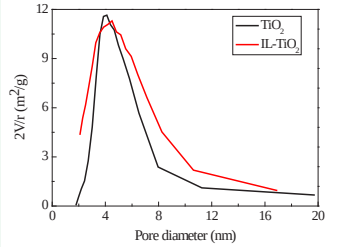

Figure 1 Pore size distribution curves of photocatalysts measured by Barrett-Joyner Halenda (BJH) method [34].

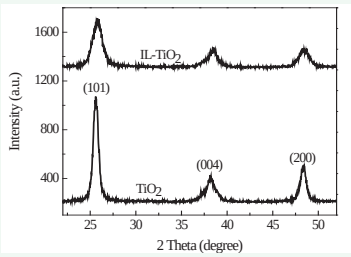

Figure 2 XRD patterns of the prepared photocatalysts.

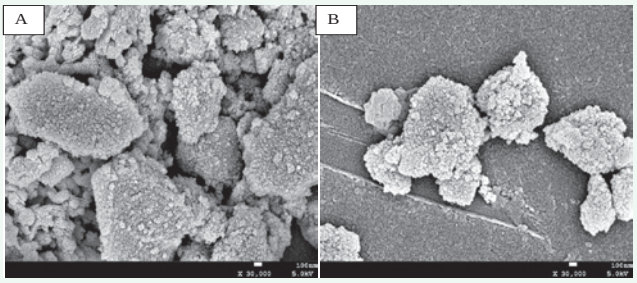

Figure 3 SEM images of photocatalysts (A) TiO_2; (B) IL-TiO_2.

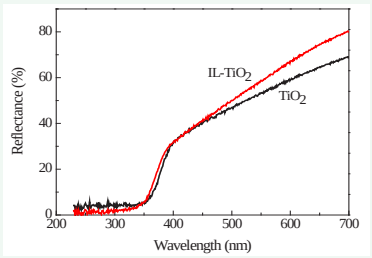

Figure 4 UV-Vis diffuse reflectance spectra of photocatalysts.

The X-ray photoelectron spectroscopy (XPS) was carried out to determine the surface chemical composition of TiO_2 and IL-TiO_2 as well as the valence states of various species. As shown in (Figure 5), the two XPS spectra reveal characteristic peaks for titanium, oxygen, and carbon. In the IL-TiO_2 XPS spectrum P and F were detected at ≤1% levels as remnants of the IL solvent on the IL-TiO_2 surface.

Figure 6 shows the high resolution XPS spectra of the $Ti2p_{3/2}$ region taken from TiO_2 and IL-TiO_2. Considering the measurement error of 0.2 eV, $Ti2p_{3/2}$ of the two photocatalysts shows no obvious difference, which suggests that no anionic doping into IL-TiO_2 and no substitution for the lattice O^{2-}.

Figure 7 shows high resolution XPS spectra of the O1s region taken on the surface of the TiO_2 and IL-TiO_2. The O1s can be fit with their curves appearing at 529.8 and 531.9 eV, which can be attributed to Ti-O (529.8 eV) and O-H (531.9 eV) components [39]. The hydroxyl groups existing on TiO_2 and IL-TiO_2 are attributable to the chemically adsorbed H_2O [39]. The adsorbed H_2O can react with TiO_2 to form Ti–OH, such as, H_2O + Ti–O–Ti → 2Ti–OH [40]. (Table 2) lists the curve-fitting results of the O1s XPS spectra for the two photocatalysts in (Figure 7) where % represents the percentage of the two kinds of oxygen contributions.

As indicated in (Table 2), the hydroxyl content on photocatalyst obtained with the addition of [BMIm]PF_6 is doubled compared to that without [BMIm]PF_6. Usually, the increase of hydroxyl content on the surface of TiO_2 is beneficial to the enhancement of photocatalytic performance in aqueous environments [40,41]. This result is then further confirmed by the results of photocatalytic activities.

The surface photovoltage (SPV) of the TiO_2 and IL-TiO_2 samples are shown in (Figure 8). As shown, the TiO_2 and IL-TiO_2 samples display obvious SPV response peaks at about 320-380

nm, which is attributed to the electronic transitions from the valence band to the conduction band (O2p → Ti3d) according to TiO_2 energy band structure and the diffuse reflectance spectroscopy.

In general, strong SPS response corresponds to high separation efficiency of photoinduced charge carriers on the basis of the SPS principle [42,43]. The strong and complex SPV signal of TiO_2 nanocrystals (NCs) indicates that TiO_2 has many trapping states. Or, in other words, photoexcited TiO_2 NCs have many surface net charges. Surface net charge potentially promotes the flow of electrons and holes. In a potential gradient this can be detected as surface current. Compared with the TiO_2 NCs, the diameter of the individual nanoparticles of IL-TiO_2 is small. The surface net charges are absent or small, and therefore, the SPV signal of IL-TiO_2 is weak. Often, higher charge separation efficiency can promote the photocatalytic performance. However, combined with the results of photocatalytic performance, it becomes obvious that the charge separation efficiency is not the decisive factor influencing the photocatalytic activity in this current case. It becomes evident that the measured surface photovoltage in TiO_2 NCs is mainly due to localized photoinduced carriers. Thus, it is interesting to study which carriers are mobile and which ones are localized. Therefore, phase spectra of TiO_2 NCs and IL-TiO_2 NCs were measured. Phase spectra of the as-prepared photocatalysts are shown in (Figure 9).

The phase values of TiO_2 are positive, which means that the photogenerated electrons transfer to the electrode from which light is incident, [44] while the phase values of IL-TiO_2 are in the negative range. This means that the photogenerated holes transport to the irradiated electrode [44]. It is clear that adding [BMIm]PF_6 into the synthesis of TiO_2 has a strong effect on the transport properties of the photogenerated charges. However, it is still unclear which element (F, P or together) or structural change caused this difference. More detailed studies will be needed in the future.

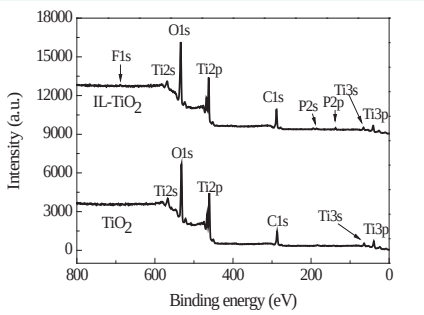

Figure 5 XPS survey spectrum for the surface of the two prepared photocatalysts.

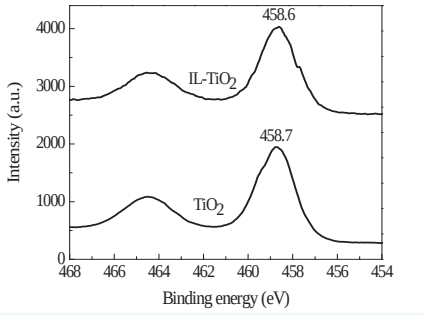

Figure 6 High resolution XPS spectra of the Ti 2p BE region of the two photocatalysts TiO_2 and IL-TiO_2. No difference in the BE of Ti ions was detected.

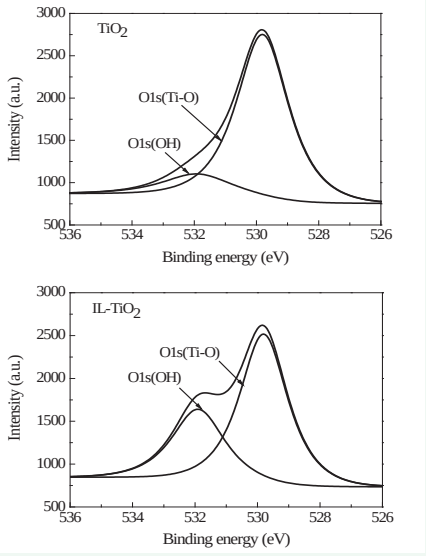

Figure 7 High resolution XPS spectra of the O1s region on the surface of two photocatalysts TiO_2 and IL-TiO_2. A much higher contribution of higher-BE oxygen is detected in IL-TiO_2, associated with more –OH groups on its surface.

Table 2: Curve-fitting results of the high resolution XPS spectra for the O1s region.

Photocatalyst	O1s (Ti-O)		O1s (O-H)	
	E_b/eV	% [a]	Eb/eV	% [a]
TiO_2	529.8	84.0	531.9	16.0
IL-TiO_2	529.8	64.8	531.9	35.2

[a] % represents the percentage $Ai/\Sigma Ai$ (Ai is the integrated area of each peak)

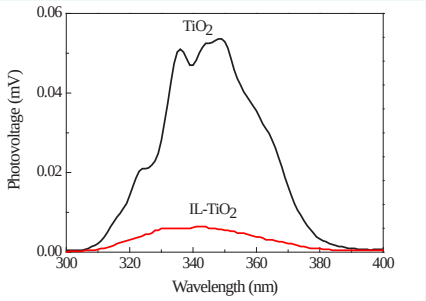

Figure 8 SPV responses of the prepared two photocatalysts.

Photocatalytic activity

Photocatalytic control experiments were carried out under two conditions: one with illumination but no photocatalysts and the other with photocatalysts (TiO_2 and IL-TiO_2) but no illumination. The results demonstrate that the decay curves of MO under the two conditions show barely any decay. The photocatalytic activities of TiO_2 and IL-TiO_2 are compared to the

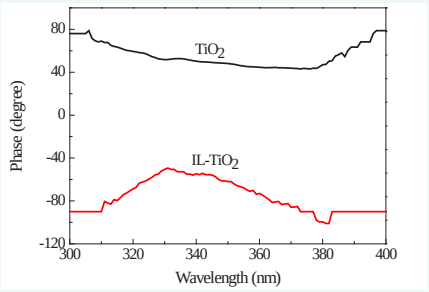

Figure 9 Phase spectra of the as-prepared photocatalysts.

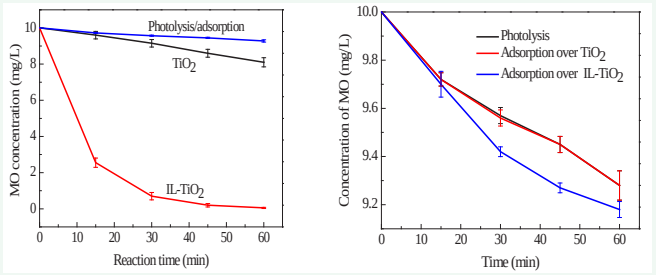

Figure 10 Conversion of methyl orange (MO) versus time. The right panel is a more detailed presentation of the non-illuminated adsorption behavior of MO on IL-TiO_2 versus TiO_2. Increased adsorption on IL-TiO_2 can be observed.

control experiments and presented in (Figure 10).

As shown in (Figure 10), the logarithmic expressions for these MO concentration curves show that the decolorization rates fit a first-order decay model well. The integral equation of $ln(C_0/C_t) = K_{obs}t$ describes the tendency, where C_0 and C_t are the concentrations of MO at time *0* and *t*, respectively, and K_{obs} is the observed pseudo first-order rate constant. The decolorization rate constant of MO solution over TiO_2 and IL-TiO_2 are 0.004 min^{-1} and 0.088 min^{-1}, respectively. The decolorization rate constant of MO solution over IL-TiO_2 is 22 times faster than over TiO_2. Adding [BMIm]PF_6 into to the synthesis dramatically promotes the photocatalytic activity of the prepared TiO_2 photocatalyst. Despite only a small increase in BET surface area (factor 1.68), the IL-based catalyst is much more photoactive (factor 22) than the one without IL addition. This is ascribed to the channel within the microporous structure of IL-TiO_2, which can facilitate access to new active sites on the catalyst walls [39]. Furthermore, the improved photocatalytic activity may be attributed to higher specific surface area, appropriate distribution of the pore size, high hydroxyl content and small nanocrystal size, as summarized above in (Table 1).

CONCLUSIONS

In conclusion, microporous TiO_2 with high photocatalytic efficient has been synthesized successively by the sol-gel method with the aid of the ionic liquid ([BMIm]PF_6). The results show that [BMIm]PF_6 not only alters the surface parameters, the morphology and the transport of the photogenerated charges, but also increases the hydroxyl content on the surface of the catalyst. The photocatalytic decolorization rate constant of MO solution over the IL-TiO_2 is 22 times of that over the reference TiO_2 photocatalyst. The unique morphology and high hydroxyl content may assist in more efficient adsorption and catalytic sites. Fabrication of TiO_2 with the assistance of ionic liquids is an effective way to promote the photocatalytic performance of nanoscale TiO2.

ACKNOWLEDGMENTS

This project was supported financially by the program of Science and Technology Department of Sichuan province (No.2013JY0080), the Project of Zigong city (10X03), Research Fund Projects of Sichuan University of Science and Engineering (2012PY05), Construct Program of the Discipline in Sichuan University of Science and Engineering, and the Opening Project of Key Laboratory of Green Catalysis of Sichuan Institutes of High Education (No. LZJ1202, LYJ1203).

REFERENCES

1. Du J, Lai X, Yang N, Zhai J, Kisailus D, Su F, et al. Hierarchically ordered macro –mesoporous TiO_2-graphene composite films: Improved mass transfer, reduced charge recombination, and their enhanced photocatalytic activities. ACS Nano. 2011; 5: 590-596.
2. Liu Y, Li J, Qiu X, Burda C. Novel TiO_2 nanocatalysts for wastewater purification: tapping energy from the sun. Water Sci Technol. 2006; 54: 47-54.
3. Liu Y, Chen X, Li J, Burda C. Photocatalytic degradation of azo dyes by nitrogen-doped TiO_2 nanocatalysts. Chemosphere. 2005; 61: 11-18.
4. Chen H, Nanayakkara CE, Grassian VH. Titanium dioxide photocatalysis in atmospheric chemistry. Chem Rev. 2012; 112: 5919-5948.
5. Linsebigler AL, Lu G, Yates JT. Photocatalysis on TiO_2 surfaces: principles, mechanisms and selected results. Chem Rev. 1995; 95: 735-758.
6. Yang L, Luo S, Li Y, Xiao Y, Kang Q, Cai Q. High efficient photocatalytic degradation of p-nitrophenol on a unique Cu2O/TiO_2 p-n heterojunction network catalyst. Environ Sci Technol. 2010; 44: 7641-7646.
7. Chang S, Lee C. A salt-assisted approach for the pore-size-tailoring of the ionic-liquid-templated TiO_2 photocatalysts exhibiting high activity. Appl Catal B: Environ. 2013; 132-133: 219-228.
8. Zhao Y, Qiu X, Burda C. The effects of sintering on the photocatalytic activity of N-doped TiO_2 nanoparticles. Chem Mater. 2008; 20: 2629-2636.
9. Qiu X, Zhao Y, Burda C. Synthesis and characterization of nitrogen-doped group IVB visible-light-photoactive metal oxide nanoparticles. Adv Mater. 2007; 19: 3995-3999.
10. Ghasemi S, Rahimnejad S, Setayesh SR, Rohani S, Gholami MR. Transition metal ions effect on the properties and photocatalytic activity of nanocrystalline TiO_2 prepared in an ionic liquid. J Hazard Mater. 2009; 172: 1573-1578.
11. Maicu M, Hidalgo MC, Colón G, Navio JA. Comparative study of the photodeposition of Pt, Au and Pd on pre-sulphated TiO_2 for the photocatalytic decomposition of phenol. J Photochem Photobiol A: Chem. 2011; 217: 275-283.
12. Kachina A, Puzenat E, Chikh SO, Geantet C, Delichere EP, Afanasiev A. New approach to the preparation of nitrogen-doped titania visible light photocatalyst. Chem Mater. 2012; 24: 636-642.
13. Hua H, Xi Y, Zhao Z, Xie X, Hu C, Liu H. Gram-scale wet chemical synthesis of Ag2O/TiO_2 aggregated sphere hetero structure with high photocatalytic activity. Mater Lett. 2013. 91: 81-83.

14. Jiao Y, Peng C, Guo F, Bao Z, Yang J, Mende LS, et al. Facile synthesis and photocatalysis of size-distributed TiO_2 hollow spheres consisting of {116} plane-oriented nanocrystallites. J Phys Chem. C 2011: 115: 6405-6409.

15. Liang YC, Wang CC, Kei CC, Hsueh YC, Cho WH, Peng TP. Photocatalysis of Ag-loaded TiO_2 nanotube arrays formed by atomic layer deposition. J Phys Chem. C 2011; 115: 9498-9502.

16. Liu Z, Li J, Ya J, Xin Y, Jin Z. Mechanism and characteristics of porous ZnO films by sol-gel method with PEG template. Mater Lett. 2008; 62: 1190-1193.

17. Zhao Q, Zhang P, Antonietti M, Yuan J. Poly(ionic liquid) complex with spontaneous micro-/mesoporosity: template-free synthesis and application as catalyst support. J Am Chem Soc. 2012; 134: 11852-11855.

18. Yoo KS, Lee TG, Kim J. Preparation and characterization of mesoporous TiO_2 particles by modified sol-gel method using ionic liquids. J Microporous Mesoporous Mater. 2005; 84: 211-217.

19. Dahl JA, Maddux BL, Hutchison JE. Toward greener nanosynthesis. Chem Rev. 2007; 107: 2228-2269.

20. Ma Z, Yu J, Dai S. Preparation of inorganic materials using ionic liquids. Adv Mater. 2010; 22: 261-285.

21. Antonietti M, Kuang D, Smarsly B, Zhou Y. Ionic liquids for the convenient synthesis of functional nanoparticles and other inorganic nanostructures. Angew Chem Int Ed Engl. 2004; 43: 4988-4992.

22. Yoo K, Choi H, Dionysiou DD. Ionic liquid assisted preparation of nanostructured TiO_2 particles. Chem Commun (Camb). 2004; : 2000-2001.

23. Wang T, Kaper H, Antonietti M, Smarsly B. Templating behavior of a long-chain ionic liquid in the hydrothermal synthesis of mesoporous silica. Langmuir. 2007; 23: 1489-1495.

24. Han CC, Ho SY, Lin YP, Lai YC, Liang WC, Yang YWC. Effect of p-p stacking of water miscible ionic liquid template with different cation chain length and content on morphology of mesoporous TiO_2 prepared via sol-gel method and the applications. Microporous Mesoporous Mater. 2010; 131: 217-223.

25. Kaper H, Sallard S, Djerdj I, Antonietti M, Smarsly BM. Toward a low-temperature Sol-Gel synthesis of TiO_2 (B) using mixtures of surfactants and ionic liquids. Chem Mater. 2010; 22: 3502-3510.

26. Zhai Y, Gao Y, Liu F, Zhang Q, Gao G. Synthesis of nanostructured TiO_2 particles in room temperature ionic liquid and its photocatalytic performance. Mater Lett. 2007; 61: 5056-5058.

27. Lu YL, Wang D, Xie T, Chen L, Lin Y. A comparative study on plate-like and flower-like ZnO nanocrystals surface photovoltage property and photocatalytic activity. Mater Chem Phys. 2011; 129: 281-287.

28. Yu JG, Zhao XJ, Zhao QN, Du JC. XPS of study of TiO_2 photocatalytic thin film prepared by the sol-gel method Chin. J Mater Res. 2000; 14: 203-209.

29. Donchev V, Kirilov K, Ivanov Ts, Germanova K. Surface photovoltage phase spectroscopy-a handy tool for characterisation of bulk semiconductors and nanostructures. K Mater Sci Eng. B 2006; 129: 186-192.

30. Li JZ, Zhong JB, Hu W, Lu Y, Zeng J, Shen YC. Fabrication of tin-doped zinc oxide by parallel flow co-precipitation with enhanced photocatalytic performance. Mater Sci Semicon Proc. 2013; 16: 143-148.

31. Zhong J, Ma D, He X, Li J, Chen Y. Sol-gel preparation and photocatalytic performance of TiO_2/SrAl2O4: Eu2+, Dy3+ toward the oxidation of gaseous benzene. J Sol-Gel Sci Technol. 2009, 52: 140-145.

32. Yang H, Shi R, Yu J, Liu R, Zhang R, Zhao H, et al. Single-crystalline ß-Ga2O3 hexagonal nanodisks: Synthesis, growth mechanism, and photocatalytic activities. J Phys Chem. C 2009; 113: 21548-21554.

33. Barrett EP, Joyner LG, Halenda PP. The determination of pore volume and area distributions in porous substances. I. Computations from nitrogen isotherms. J Am Chem Soc. 1951; 73: 373-380.

34. Lin YP, Chen YY, Lee YC, Chen-Yang YW. Effect of wormhole-like mesoporous anatase TiO_2 nanofiber prepared by electrospinning with ionic liquid on dye-sensitized solar cells. J Phys Chem. C 2012; 116: 13003-13012.

35. Liu Y, Li J, Wang M, Li Z, Liu H, He P, et al. Preparation and properties of nanostructure anatase TiO_2 monoliths using 1-Butyl-3-methylimidazolium Tetrafluoroborate room-temperature ionic liquids as template solvents. J Cryst Growth Des. 2005; 5: 1643-1649.

36. Yoo KS, Lee TG, Kim J. Preparation and characterization of mesoporous TiO_2 particles by modified sol-gel method using ionic liquids. Microporous Mesoporous Mater. 2005; 84: 211-217.

37. Choi H, Kim YJ, Varma RS, Dionysiou DD. Thermally stable nanocrystalline TiO_2 photocatalysts synthesized via Sol-Gel methods modified with ionic liquid and surfactant molecules. Chem Mater. 2006; 18: 5377-5384.

38. Burda C, Chen X, Narayanan R, El-Sayed MA. Chemistry and properties of nanocrystals of different shapes. Chem Rev. 2005; 105: 1025-1102.

39. Yu JC, Yu J, Zhao J. Enhanced photocatalytic activity of mesoporous and ordinary TiO_2 thin films by sulfuric acid treatment. Appl Catal B: Environ. 2002; 36: 31-43.

40. Yu J, Zhao X. Effect of surface treatment on the photocatalytic activity and hydrophilic property of the sol-gel derived TiO_2 thin films. Mater Res Bull. 2001; 36: 97-107.

41. Hoffmann MR, Martin ST, Choi W, Bahnemann DW. Environmental applications of Semiconductor Photocatalysis. Chem Rev. 1995; 95: 69-96.

42. Jing LQ, Wang J, Qu Y, Luan Y. Effects of surface-modification with Bi2O3 on the thermal stability and photoinduced charge property of nanocrystalline anatase TiO_2 and its enhanced photocatalytic activity. Appl Surf Sci. 2009; 256: 657-663.

43. Mohapatra L, Parida K, Satpathy M. Molybdate/Tungstate intercalated oxo-bridged Zn/Y LDH for solar light induced photodegradation of organic pollutants. J Phys Chem. C 2012; 116: 13063-13070.

44. Zhao Q, Xie T, Peng L, Lin Y, Wang P, Peng L, et al. Size- and orientation-dependent photovoltaic properties of ZnO nanorods. J Phys Chem. C 2007; 111: 17136-17145.

Cite this article

Zhong J, Li JZ, Feng F, Huang S, Jiang W, et al. (2013) Ionic Liquid-Assisted Fabrication of Nanoscale Microporous TiO_2 with Enhanced Photocatalytic Performance. JSM Nanotechnol Nanomed 1(2): 1015.